第 34 卷第 4 期
2017 年 4 月

控 制 理 论 与 应 用
Control Theory & Applications

Vol. 34 No. 4
Apr. 2017

DOI: 10.7641/CTA.2017.16016

基于滚动时域优化的轮式移动机器人路径跟踪问题研究

刘　洋[1,2], 于树友[1,3†], 郭　洋[1], 高炳钊[3], 陈　虹[1,3]

(1. 吉林大学 控制科学与工程系, 吉林 长春 130012;
2. 中国第一汽车股份有限公司技术中心, 吉林 长春 130000;
3. 吉林大学 汽车仿真与控制国家重点实验室, 吉林 长春 130012)

摘要: 轮式移动机器人是典型的非完整约束系统. 本文基于滚动时域控制策略研究轮式移动机器人的路径跟踪问题. 为了既能够保证移动机器人渐近收敛到期望轨迹, 又能够保证在线求解的优化问题的滚动可行性, 参考轨迹被选为优化问题中的终端等式约束. 仿真结果验证了所提出的控制策略的有效性.

关键词: 模型预测控制; 非线性约束系统; 轮式移动机器人; 路径跟踪问题

中图分类号: TP273　　**文献标识码**: A

Receding horizon control for path following problems of wheeled mobile robots

LIU Yang[1,2], YU Shu-you[1,3†], GUO Yang[1], GAO Bing-zhao[3], CHEN Hong[1,3]

(1. Department of Control Science and Engineering, Jilin University, Changchun Jilin 130012, China;
2. China FAW Group Corporation R&D Center, Changchun Jilin 130000, China;
3. State Key Laboratory of Automotive Simulation and Control, Jilin University, Changchun Jilin 130012, China)

Abstract: A wheeled mobile robot is a system with nonholonomic constraints, which path following problems have been studied intensively. Receding horizon control for path following problems of wheeled mobile robots is considered in this paper, where the reference path is chosen as the terminal region. Both the asymptotic convergence to the reference path and recursive feasibility of the involved optimization problem are investigated. The effectiveness of the applied control strategy is verified by simulation results.

Key words: model predictive control; constrained nonlinear systems; wheeled mobile robots; path following problems

1 Introduction

There are three fundamental motion control problems in the control field, namely the set-point stabilization, trajectory tracking and path following. Set-point stabilization, as a classical regulation problem, is to regulate the state of the system to a fixed target state[1]. Trajectory tracking (TT) aims at tracking a given time varying reference trajectory, which is a time parameterized curve[2]. Path following (PF) is regarded as an alternative problem formulation to trajectory tracking. PF is also to guarantee the system to follow a reference path, but the reference path is parameterized in its geometrical coordinates instead.

The differences between the TT and PF are in the following aspects: 1) TT problem has strict requirements on time, PF is allowed to determine velocity online; 2) The reference trajectory is highly dependent on the reference model in TT problem; 3) Following a parameterized reference path means to design a controller which affects both the system behavior and the evolution of the reference path[3].

Path following is widely applied in (automobile, ship or flight) course control[4], car-parking problem or the control of robots[5–6], and batch crystallization[7]. Accordingly, many different PF control schemes have been exploited. For example, path following was developed by feedforward control scheme in [8–9], transverse feedback linearization techniques in [10], backstepping designs in [11–12], sliding mode control in [13–14] and other advanced control algorithms in [15–16]. These controllers are either restricted for application or limited in the fact that the state and input constraints are not considered. Recent papers about control of robots are concerned with the input saturation or output constraint problem[17–18].

Since receding horizon control, also referred to as model predictive control (MPC), can handle the control problems for nonlinear systems subject to state and in-

Received 24 January 2016; accepted 17 February 2017.
†Corresponding author. E-mail: shuyou@jlu.edu.cn; Tel.: +86 431-85095243.
Recommended by Associate Editor LI Zhi-jun.
Supported by National Natural Science Foundation of China (61573165, 61520106008).

put constraints, it has become one of the most standard and frequently used techniques recently. In general, at each sampling instant, MPC scheme solves a finite horizon open-loop optimization problem based on the current state of system, and finds a control sequence, then applies the first control action to the system. MPC has achieved rich results in stability, robustness and optimality analysis, and has formed mature scientific analysis and design methods[19–21]. Many exhaustive results on MPC for regulation problems are available. Trajectory tracking control scheme with MPC has also been discussed, but quite a lot literatures only considered tracking the piecewise constant references, as in [22–23]. Although many researchers have applied MPC framework to solve the PF problems[24–26], these schemes are either only fit for the given systems or rely on some certain characteristics of systems, for example, the property of differential flatness.

Normally, stability of MPC is achieved by adding a terminal penalty to the cost function and restricting terminal state to a terminal region. But it is usually difficult or time-consuming to calculate the suitable terminal ingredients. The terminal ingredients are locally defined which will lead to a potentially restricted region of attraction. Therefore many approaches for calculating the terminal region have been proposed as in [27] and references therein. However, [28] has proved that forcing the terminal state to equal zero can guarantee stability. In this paper a receding horizon MPC scheme is proposed to solve PF problem of a wheeled mobile robot. Since the reference path is chosen as the terminal region it can avoid the complex calculation of the suitable terminal ingredients.

This paper is organized as follows. The kinematics model of a nonholonomic mobile robot is described in Section 2. Section 3 first introduces both the path following problem and MPC scheme for path following problems which chooses the reference path as the terminal region. Then, feasibility of the involved optimization problem is presented. The simulation implementation of the mobile robot is provided in Section 4. Finally, a brief summary is given in Section 5.

Notations and Definitions:

$\mathbb{R}^n$ is the n-dimensional Euclidean space of real valued vectors. Let I denote the field of non-negative integers, I_+ the field of positive integers. The norm $\|x\|_Q$ of $x\in\mathbb{R}^n$ denotes $\|x\|_Q=\sqrt{x^{\mathrm{T}}Qx}$, $Q\in\mathbb{R}^{n\times n}$, $Q>0$. $x_{k|k}(k\in I)$ denotes the measured value of variable x at time instant k. $x_{k+i|k}(i\in I_+)$ denotes the predicted value of x at future time instant $k+i$ predicted at real time instant k.

2 Path following problems of robots

The nonholonomic wheeled mobile robot has a front castor and two rear driving wheels, which is shown in the world coordinate system, cf. Fig.1. The corresponding symbols are described in Table 1.

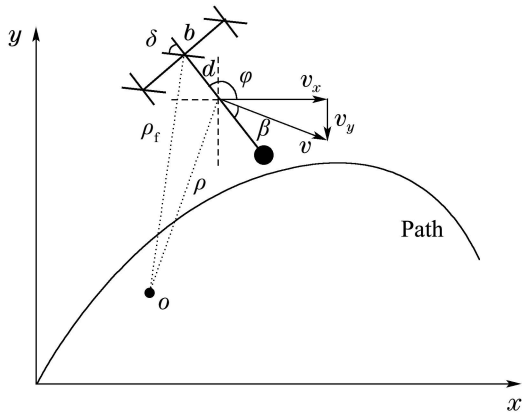

Fig. 1 The simplified model of a wheeled mobile robot

Table 1 The description for symbol definitions

Parameter	Symbol
Track between front wheels	$2b$
Vertical distance between centroid and front wheel	d
The radius of the wheel	r
Instantaneous center of robot	O
Distance between instantaneous center and the front wheel	ρ_{f}
Distance between instantaneous center and the centroid	ρ
Resultant velocity of the centroid	v
Side slip angle	β
Yaw angle	ϕ
Steering angle	δ
Steering angle	w_{l}
The velocity of the left wheel	w_{f}

According to the geometric relationship shown in Fig.1, the distance between instantaneous center and front wheel, and the distance between instantaneous center and centroid are

$$\rho_{\mathrm{f}}=\frac{\omega_{\mathrm{r}}+\omega_{\mathrm{l}}}{\omega_{\mathrm{r}}-\omega_{\mathrm{l}}}b, \tag{1a}$$

$$\rho=\sqrt{(\rho_{\mathrm{f}}\sin\delta-d)^2+(\rho_{\mathrm{f}}\cos\delta)^2}. \tag{1b}$$

The yaw rate of the wheeled mobile robot is given by

$$\dot{\varphi}=\frac{\frac{\omega_{\mathrm{r}}+\omega_{\mathrm{l}}}{2}r}{\rho_{\mathrm{f}}}=\frac{r}{2b}(\omega_{\mathrm{r}}-\omega_{\mathrm{l}}). \tag{2}$$

Thus the resultant velocity of the centroid is

$$v=\rho\dot{\varphi}=\frac{r(\omega_{\mathrm{r}}-\omega_{\mathrm{l}})}{2b}\sqrt{(\rho_{\mathrm{f}}\sin\delta-d)^2+(\rho_{\mathrm{f}}\cos\delta)^2}. \tag{3}$$

The state of the robot is described by vector $(x,y,\varphi)^{\mathrm{T}}$, which includes its position (x,y) and orientation φ. Therefore, the kinematics equation, while the tire deformation is neglected, is as follows:

$$\begin{bmatrix}\dot{x}\\ \dot{y}\\ \dot{\varphi}\end{bmatrix} = \begin{bmatrix} v\cos(\beta+\varphi)\\ v\sin(\beta+\varphi)\\ r\cdot(\omega_{\rm r}-\omega_{\rm l})/2b\end{bmatrix}, \tag{4}$$

where

$$\beta = \arctan\frac{\rho_{\rm f}\sin\delta - d}{\rho_{\rm f}\cos\delta}.$$

In order to verify the effectiveness of the proposed robot model, let us consider the case of $\delta = 0$. While $\delta = 0$,

$$\begin{cases}\sin\beta = \dfrac{d}{\rho},\\ \cos\beta = \dfrac{\rho_{\rm f}}{\rho},\\ v = \dfrac{\rho}{\rho_{\rm f}}\dfrac{(\omega_{\rm r}+\omega_{\rm l})}{2}r.\end{cases} \tag{5}$$

By means of trigonometric functions and Eq.(6), we can get

$$\begin{cases}\dot{x} = \dfrac{\cos\varphi}{2}r(\omega_{\rm r}+\omega_{\rm l}) - \dfrac{\sin\varphi}{2b}rd(\omega_{\rm r}-\omega_{\rm l}),\\ \dot{y} = \dfrac{\sin\varphi}{2}r(\omega_{\rm r}+\omega_{\rm l}) - \dfrac{\cos\varphi}{2b}rd(\omega_{\rm r}-\omega_{\rm l}),\\ \dot{\varphi} = \dfrac{r}{2b}(\omega_{\rm r}-\omega_{\rm l}),\end{cases} \tag{6}$$

which is the same as the kinematics equation of the mobile robot without steering[29].

Equation (5) is too complex to design controllers. Particularly, choose δ such that

$$\rho_{\rm f}\sin\delta - d = 0. \tag{7}$$

Thus, Eq.(5) can be transformed into

$$\begin{bmatrix}\dot{x}\\ \dot{y}\\ \dot{\varphi}\end{bmatrix} = \begin{bmatrix} v\cos\varphi\\ v\sin\varphi\\ w\end{bmatrix}, \tag{8}$$

where $\beta = 0, v = \dfrac{r}{2}(\omega_{\rm r}+\omega_{\rm l})\cos\delta, w = \dfrac{r}{2b}(\omega_{\rm r}-\omega_{\rm l})$. The term w can be seen as the angular velocity of the yaw angle.

Remark 1 $\beta = 0$ in Eq.(9) will improve maneuverability of robots. Furthermore, there is no any singular point when $\omega_{\rm r}-\omega_{\rm l} = 0$.

Assume that there is a virtual mobile robot moving along the reference path, which position and orientation represent the ideal state of the robot. Denote $(x_R, y_R, \varphi_R)^{\rm T}$ as a reference state

$$\begin{bmatrix}\dot{x}_R\\ \dot{y}_R\\ \dot{\varphi}_R\end{bmatrix} = \begin{bmatrix} v_R\cos\varphi_R\\ v_R\sin\varphi_R\\ w_R\end{bmatrix}. \tag{9}$$

Denote $(x_{\rm e}, y_{\rm e}, \varphi_{\rm e})^{\rm T}$ as the error state which represents the deviation of the current position to the reference. Under the virtual reference robot coordinate system, the error state is as follows:

$$\begin{bmatrix}x_{\rm e}\\ y_{\rm e}\\ \varphi_{\rm e}\end{bmatrix} = \begin{bmatrix}\cos\varphi & \sin\varphi & 0\\ -\sin\varphi & \cos\varphi & 0\\ 0 & 0 & 1\end{bmatrix}\begin{bmatrix}x_R - x\\ y_R - y\\ \varphi_R - \varphi\end{bmatrix}. \tag{10}$$

Furthermore, the error dynamic is

$$\begin{bmatrix}\dot{x}_{\rm e}\\ \dot{y}_{\rm e}\\ \dot{\varphi}_{\rm e}\end{bmatrix} = \begin{bmatrix} wy_{\rm e} - v + v_R\cos\varphi_{\rm e}\\ -wx_{\rm e} + v_R\sin\varphi_{\rm e}\\ w_R - w\end{bmatrix}. \tag{11}$$

Note that when v and w approach v_R and w_R respectively, the error state, $(x_{\rm e}, y_{\rm e}, \varphi_{\rm e})^{\rm T}$, is close to the equilibrium, c.f. Eq.(12).

Remark 2 Sometimes the control signal in the control for path following problems of wheeled mobile robots is chosen as $u' = (w_{\rm l}, w_{\rm r}, \delta)^{\rm T}$, see Eq.(5). Using Eq.(8), the relationship between u and u' is

$$\begin{cases} r(\omega_{\rm r}+\omega_{\rm l})\cos\delta = 2v,\\ r(\omega_{\rm r}-\omega_{\rm l}) = 2bw,\\ \dfrac{(\omega_{\rm r}-\omega_{\rm l})}{(\omega_{\rm r}+\omega_{\rm l})}\dfrac{d}{b} = \sin\delta,\end{cases} \tag{12}$$

where r, b, d are the given parameters of the wheeled mobile robot, i.e., Table 1.

The task for path following problems of a wheeled mobile robot can be described as: Given a reference path, find an admissible control law $u = (v, w)^{\rm T}$ which drives the error state $(x_{\rm e}, y_{\rm e}, \varphi_{\rm e})^{\rm T}$ to zero.

3 Receding horizon control for path following problems

Consider a discrete-time nonlinear system

$$x_{k+1} = f(x_k, u_k),\ k \in I, \tag{13}$$

where $x_k \in \mathbb{R}^n$ and $u_k \in \mathbb{R}^m$ are the system state and input at time instant k. The constraints of the system state and input described by sets X and U are as follows:

$$x_k \in X,\ u_k \in U.$$

The nonlinear function $f : \mathbb{R}^n \times \mathbb{R}^m \to \mathbb{R}^n$ is locally Lipchitz with respect to both x_k and u_k.

Assumption 1 $U \subseteq \mathbb{R}^m$ is compact and convex, and $X \subseteq \mathbb{R}^n$ is closed and connected. The origin $(0, 0)$ contains in its interior.

The objective of path following problems is to make system state x_k to follow a parameterized reference path, which is defined in the state space by a scalar θ_k

$$P = \{\, r_k \in \mathbb{R}^n |\ r_k = p(\theta_k)\,\}. \tag{14}$$

The map $p : \mathbb{R}^1 \to \mathbb{R}^n$ is a twice continuously differentiable function. The scalar $\theta_k \in \Theta \subseteq \mathbb{R}^1$ is not given a priori but specified by a virtual input

$$\theta_{k+1} = g(\theta_k, v_k),\ v_k \in V \subseteq \mathbb{R}^1, \tag{15}$$

where Θ and V are compact sets.

Assumption 2 The reference path P is contained in the state constraint set, i.e., $P \subseteq X$.

Assumption 3 $g(\theta_k, v_k)$ in Eq.(16) has the same requirements as $f(x_k, u_k)$, i.e., $g : \mathbb{R}^1 \times \mathbb{R}^1 \to \mathbb{R}^1$ is locally Lipchitz with respect to both θ_k and v_k. Besides, $g(\theta_k, v_k) > 0$ for all $v_k \in V$ and for all $\theta_k \in \Theta$.

Define the error state

$$\tilde{x}_k := x_k - p(\theta_k). \tag{16}$$

Then, the error state dynamic model is

$$\tilde{x}_{k+1} = f(x_k, u_k) - p(g(\theta_k, v_k)). \tag{17}$$

So the path following problems can be reduced to find admissible inputs u_k, v_k and θ_k such that the system state x_k could converge to the reference, i.e., $\lim\limits_{k\to\infty} \tilde{x}_k = 0$, and the constraints $x_k \in X, u_k \in U, \theta_k \in \Theta$ and $v_k \in V$ are satisfied for all k.

Redefine a control input $\tilde{u}_k \in \tilde{U} \subseteq \mathbb{R}^m$ and a function $F(\cdot,\cdot)$ of the error state dynamic model, Eq.(18) can be rewritten as

$$\tilde{x}_{k+1} := F(\tilde{x}_k, \tilde{u}_k). \tag{18}$$

Assumption 4 There exist admissible inputs $u_k \in U$ and $v_k \in V$ such that the state $x_k \in X$ and the path parameter $\theta_k \in \Theta$ satisfy $\tilde{x}_{k+1} = 0$ while $\tilde{x}_k$ equals to zero.

3.1 MPC scheme with terminal inequality constraints

To solve the above considered path following problem, a nonlinear model predictive framework is proposed[30]. At each time instant k, the following optimization problems are solved:

Problem 1

$$\underset{u_{k+i|k}, v_{k+i|k}, \theta_{k+i|k}}{\text{minimize}} \quad J(x_{k|k},\ u_{k+i|k}, v_{k+i|k}, \theta_{k+i|k}), \tag{19a}$$

subject to

$$x_{k+i+1|k} = f(x_{k+i|k}, u_{k+i|k}),\ x_{k|k} = x_k, \tag{19b}$$

$$x_{k+i|k} \in X,\ u_{k+i|k} \in U, \tag{19c}$$

$$\tilde{x}_{k+i|k} = x_{k+i|k} - p(\theta_{k+i|k}), \tag{19d}$$

$$\tilde{x}_{k+N|k} \in \Omega, \tag{19e}$$

$$\theta_{k+i+1|k} = g(\theta_{k+i|k}, v_{k+i|k}),\ \theta_{k|k} = \theta_k, \tag{19f}$$

$$\theta_{k+i|k} \in \Theta,\ v_{k+i|k} \in V, \tag{19g}$$

where

$$J(\tilde{x}_{k+i|k}, \tilde{u}_{k+i|k}) = \mathrm{E}(\tilde{x}_{k+N|k}) + \sum_{i=0}^{N-1} (\|\tilde{x}_{k+i|k}\|_Q^2 + \|\tilde{u}_{k+i|k}\|_R^2), \tag{20}$$

with Q and R are positive definite weight matrices, and N is the prediction horizon.

The terminal penalty $E(\tilde{x}_{k+N|k})$ and the terminal region Ω are adopted to guarantee the recursive feasibility of the optimization problem and asymptotic convergence of the system dynamics to the reference path. The terminal inequality constraint Eq.(19e) denotes that the predicted state $x_{k+i|k}$ has to be restricted inside it at the end of each prediction.

Besides the standard constraints (19b)–(19e), the extra path following constraints (19f) and (19g) describe the evolution of the reference path P, which is parameterized in its path parameter θ_k. The sequence of θ_k will be determined online so as to make error as small as possible. The virtual input v_k controls the evolution of the path parameter θ_k, which is an extra determined variable in the MPC scheme.

Remark 3 Note that the initial value of θ_k is another determined variable of Problem 1. In other words, the initial condition θ_0 is also determined online to make $J(x, u, v, \theta)$ as small as possible. If no initial path point is given, another method in [3] to get θ_0 is proposed to find a path point close to the initial state x_0 by solving

$$\underset{\theta_0}{\text{minimize}} \ \|x_0 - p(\theta_0)\|. \tag{21}$$

In general, a suitable terminal penalty $E(\tilde{x})$, a terminal region Ω and a terminal control law $u_{\mathrm{F}}(\tilde{x})$ are adopted to guarantee recursive feasibility and asymptotic convergence of the proposed MPC scheme. The terminal control law is used to calculate $E(\tilde{x})$ and Ω, but not directly applied to the system. In the standard MPC framework, the specific form of $E(\tilde{x})$ is usually defined as follows

$$E(\tilde{x}) = \tilde{x}^{\mathrm{T}} P \tilde{x}, \tag{22}$$

where P is a terminal penalty matrix. P is a positive definite solution of a Lyapunov equation for a given linear state feedback gain[31]. Then the corresponding terminal region Ω is defined

$$\Omega := \{\tilde{x} \in \mathbb{R}^n \,|\, \tilde{x}^{\mathrm{T}} P \tilde{x} \leqslant \alpha\}, \tag{23}$$

where α is a positive scalar. These terminal ingredients should satisfy some sufficient conditions which are shown in the following theorem.

Theorem 1 Suppose that

- Assumption 1 – Assumption 4 are satisfied.
- $u_{\mathrm{F}}(\tilde{x}) \in \tilde{U}$ for all $\tilde{x} \in \Omega \subseteq X$. Furthermore, $u_{\mathrm{F}}(0) = 0$.
- For all $\tilde{x} \in \Omega$ and $k > 0$, $E(\tilde{x})$ satisfies

$$E(\tilde{x}_{k+1+N|k+1}) - E(\tilde{x}^*_{k+N|k}) + \left\|\tilde{x}_{k+N|k+1}\right\|_Q^2 + \left\|\tilde{u}_{k+N|k+1}\right\|_R^2 \leqslant 0, \tag{24}$$

- Problem 1 is feasible at the initial time instant.

Then,

1) Problem 1 has a feasible solution for all $k > 0$.

2) The error $\tilde{x}$ can converge to zero as $k \to \infty$, i.e., system (14) can follow the given path as $k \to \infty$.

Proof Suppose that at time instant k, Problem 1 has a feasible solution $\tilde{U}^*_k \in \tilde{U}$,

$$\tilde{U}^*_k = [\tilde{u}^*_{k|k}\ \ \tilde{u}^*_{k+1|k}\ \ \cdots\ \tilde{u}^*_{k+N-1|k}], \tag{25}$$

the corresponding error trajectory is denoted as $\tilde{X}^*_k$,

$$\tilde{X}_k^* = [\tilde{x}_{k|k}^* \ \ \tilde{x}_{k+1|k}^* \ \ \cdots \ \tilde{x}_{k+N|k}^*]. \quad (26)$$

The related cost function $V_k(\tilde{x}, \tilde{u})$ is

$$V_k(\tilde{x}, \tilde{u}) := J_k = \sum_{i=0}^{N-1} (\|\tilde{x}_{k+i|k}^*\|_Q^2 + \|\tilde{u}_{k+i|k}^*\|_R^2) + E(\tilde{x}_{k+N|k}^*). \quad (27)$$

Apply $\tilde{u}_k = \tilde{u}_{k|k}^*$ to the system (14). Since neither model mismatches nor external disturbances is considered, the error system state at time instant $k+1$ is the same as $\tilde{x}_{k+1|k}^*$. Therefore, a feasible solution to Problem 1 can be chosen as

$$\tilde{U}_{k+1} = [\tilde{u}_{k+1|k}^* \ \cdots \ \tilde{u}_{k+N-1|k}^* \ \ u_{\rm F}(\tilde{x}_{k+N|k}^*)]. \quad (28)$$

$\tilde{U}_{k+1}$ can be understood as a sequence which concatenates the shifted optimal input $\tilde{U}_k^*$ with the terminal control law $u_{\rm F}$. In terms of $\tilde{x}_{k+N|K}^* \in \Omega$, $u_{\rm F}(\tilde{x}_{k+N|k}^*) \in \tilde{U}$, $\tilde{U}_{k+1}$ satisfies the input constraint, which implies Problem 1 is feasible at time instant $k+1$ if Problem 1 has a feasible solution at time instant k. Under the control sequence $\tilde{U}_{k+1}$, the state sequence $\tilde{X}_{k+1}$ is

$$\tilde{X}_{k+1} = [\tilde{x}_{k+1|k}^* \ \cdots \ \tilde{x}_{k+N|k}^* \ \ \tilde{x}_{k+N+1|k+1}], \quad (29)$$

which satisfies the state constraint and terminal constraint. The cost function at time instant $k+1$ is

$$\begin{aligned} J_{k+1} = & \sum_{i=0}^{N-1} (\|\tilde{x}_{k+1+i|k+1}\|_Q^2 + \|\tilde{u}_{k+1+i|k+1}\|_R^2) + \\ & E(\tilde{x}_{k+1+N|k+1}) = \\ & \sum_{i=1}^{N-1} (\|\tilde{x}_{k+1+i|k}^*\|_Q^2 + \|\tilde{u}_{k+1+i|k}^*\|_R^2) + \\ & \|\tilde{x}_{k+N|k+1}\|_Q^2 + \|\tilde{u}_{k+N|k+1}\|_R^2 + \\ & E(\tilde{x}_{k+1+N|k+1}) = \\ & \sum_{i=0}^{N-1} (\|\tilde{x}_{k+i|k}^*\|_Q^2 + \|\tilde{u}_{k+i|k}^*\|_R^2) - \\ & \|\tilde{x}_{k|k}^*\|_Q^2 - \|\tilde{u}_{k|k}^*\|_R^2 + \|\tilde{x}_{k+N|k+1}\|_Q^2 + \\ & \|\tilde{u}_{k+N|k+1}\|_R^2 + E(\tilde{x}_{k+1+N|k+1}), \end{aligned}$$

since the optimal solution at time instant $k+1$ is better than the feasible solution $\tilde{U}_{k+1}$, i.e., $V_{k+1} \leqslant J_{k+1}$. Thus

$$\begin{aligned} & V_{k+1} - V_k \leqslant J_{k+1} - J_k = \\ & -\|\tilde{x}_{k|k}^*\|_Q^2 - \|\tilde{u}_{k|k}^*\|_R^2 + \|\tilde{x}_{k+N|k+1}\|_Q^2 + \\ & \|\tilde{u}_{k+N|k+1}\|_R^2 + E(\tilde{x}_{k+1+N|k+1}) - E(\tilde{x}_{k+N|k}^*). \end{aligned} \quad (30)$$

Due to Eq.(25),

$$V_{k+1} - V_k \leqslant -\|\tilde{x}_{k|k}^*\|_Q^2 - \|\tilde{u}_{k|k}^*\|_R^2. \quad (31)$$

Clearly, the value function V_k is monotonically decreasing and has zero as its low bound. Then the state trajectory of system (14) will converge to the reference path, i.e., $\lim\limits_{k\to\infty} \tilde{x}_k = 0$.

3.2 MPC scheme with terminal equality constraints

To find suitable terminalpenalty $E(\cdot)$, terminal region Ω, and terminal control law $u_{\rm F}$, which is required by Theorem 1, is an important part of the MPC scheme. Unfortunately, it is usually difficult to calculate these terminal ingredients. In the following the reference path P is chosen as terminal region Ω. In other words, the terminal region is defined as follows:

$$\Omega := \{0\}. \quad (32)$$

Eq.(33) indicates the error $\tilde{x}$ of path following problem will be forced to equal zero at the end of each prediction. Compared to Eq.(24), Eq.(33) is essentially a terminal equality constraint. At the same time, forcing the terminal state to be equal to zero makes the terminal penalty and the terminal control law unnecessary in achieving the convergence of the MPC scheme. So the terminal penalty and the terminal control law are chosen as $E(\cdot) = 0$ and $u_{\rm F} = 0$.

Therefore, when Eq.(19e) in Problem 1 is replaced by Eq.(33), the MPC scheme with terminal equality constraints is obtained.

Problem 2

$$\underset{u_{k+i|k}, v_{k+i|k}, \theta_{k+i|k}}{\text{minimize}} \ J(x_{k|k}, \ u_{k+i|k}, v_{k+i|k}, \theta_{k+i|k}), \quad (33)$$

subject to

$$x_{k+i+1|k} = f(x_{k+i|k}, u_{k+i|k}), \ x_{k|k} = x_k, \quad (34a)$$

$$x_{k+i|k} \in X, \ u_{k+i|k} \in U, \quad (34b)$$

$$\tilde{x}_{k+i|k} = x_{k+i|k} - p(\theta_{k+i|k}), \quad (34c)$$

$$\tilde{x}_{k+N|k} = 0, \quad (34d)$$

$$\theta_{k+i+1|k} = g(\theta_{k+i|k}, v_{k+i|k}), \ \theta_{k|k} = \theta_k, \quad (34e)$$

$$\theta_{k+i|k} \in \Theta, \ v_{k+i|k} \in V, \quad (34f)$$

where

$$J(\tilde{x}_{k+i|k}, \ \tilde{u}_{k+i|k}) = \sum_{i=0}^{N-1} (\|\tilde{x}_{k+i|k}\|_Q^2 + \|\tilde{u}_{k+i|k}\|_R^2). \quad (35)$$

The following corollary shows that asymptotic convergence to the reference path is guaranteed by the calculation of Problem 2 at each time instant.

Corollary 1 (Zero terminal region for MPC) Suppose that

- Assumptions 1–4 are satisfied.
- Problem 2 has a feasible solution at $k = 0$.

Then,

1) Problem 2 is feasible for all time instants $k > 0$.

2) The state trajectory of the system converges to the reference path as $k \to \infty$.

Sketch of Proof Let $\tilde{U}_k^*, \tilde{X}_k^*$ in Eq.(26) and Eq.(27) denote the control input and the error state at time instant k. Moreover, owing to the terminal equality constraint Eq.(33),

$$\tilde{X}_k^* = [\tilde{x}_{k|k}^* \ \ \tilde{x}_{k+1|k}^* \ \cdots \ \tilde{x}_{k+N|k}^*] = [\tilde{x}_{k|k}^* \ \ \tilde{x}_{k+1|k}^* \ \cdots \ 0].$$

Note that the control input $\tilde{U}_k^*$ forces the terminal state (the state at time $k+N$) to zero.

At time instant $k+1$, a feasible input sequence is

$$\tilde{U}_{k+1} = [\tilde{u}^*_{k+1|k} \ \cdots \ \tilde{u}^*_{k+N-1|k} \ \ 0].$$

Since neither model mismatches nor external disturbances exists, in accordance with $\tilde{U}_{k+1}$, the state sequence $\tilde{X}_{k+1}$ is

$$\tilde{X}_{k+1} = [\tilde{x}^*_{k+1|k} \ \ \tilde{x}^*_{k+2|k} \ \cdots \ \tilde{x}^*_{k+N|k} \ \ \tilde{x}_{k+N+1|k+1}] = [\tilde{x}^*_{k+1|k} \ \ \tilde{x}^*_{k+2|k} \ \cdots \ 0].$$

Due to Assumption 2 and Assumption 4, system (14) can follow the reference path while $\tilde{x}_k = 0$. Since $\tilde{x}_{k+N|k+1} = 0$ and $\tilde{u}_{k+N|k+1} = 0$,

$$V_{k+1} - V_k \leqslant J_{k+1} - J_k = -\|\tilde{x}^*_{k|k}\|^2_Q - \|\tilde{u}^*_{k|k}\|^2_R.$$

The sequence J_k is therefore nonincreasing and bounded below by zero. Therefore the error $\tilde{x}$ converges to zero as $k \to \infty$.

4 Simulations

In order to verify the effectiveness of the MPC scheme with terminal equality constraint (zero terminal region), path following problems of wheeled mobile robots are considered. Furthermore, both the system dynamics and computational burden of MPC scheme with terminal inequality constraints are provided under the same simulation conditions, i.e., Table 2.

Table 2 The conditions for simulation

Parameter	Value
Prediction horizon	$N = 10$
Sampling time	$\delta = 0.2$ s
Weight matrices	$Q = \mathrm{diag}\{0.5, 0.5, 0.5\}$ $R = \mathrm{diag}\{0.5, 0.5\}$
Mechanical parameters	$r = 80$ mm $2b = 460$ mm $d = 750$ mm
Input constraints	$0 \leqslant v \leqslant 3$ m/s $-3.5 \leqslant w \leqslant 3.5$ rad/s
Initial state	$x_0 = [-0.4, -0.8, \pi/2]^{\mathrm{T}}$

Three kinds of reference paths are adopted to test the performance of the receding horizon control for path following problems. The terminal inequality constraints are calculated by using the methods proposed in [30], where vertexes of the polytypic linear differential inclusion of the three paths are chosen the same in order to get the unified terminal ingredients. The obtained terminal inequality constraint is

$$\Omega := \{\tilde{x} \in \mathbb{R}^3 \mid \tilde{x}^{\mathrm{T}} P \tilde{x} \leqslant \alpha\},$$

where $\alpha = 25$ and

$$P = \begin{bmatrix} 26.03 & 0 & 0 \\ 0 & 28.11 & 7.49 \\ 0 & 7.49 & 26.50 \end{bmatrix}.$$

4.1 Eight-shaped path

The first path is an eight-shaped path, where

$$x_R = 1.8\sin\theta, \ \ y_R = 1.2\sin(2\theta). \tag{36}$$

The simulation results are shown in Figs.2–4. Both MPC scheme with zero terminal region and MPC scheme with non-zero terminal region are capable of driving the robot to follow the reference eight-shaped curve, and MPC scheme with zero terminal region can achieve a better performance (smaller error). But the computational time of MPC scheme with zero terminal region increases accordingly, c.f. Table 3.

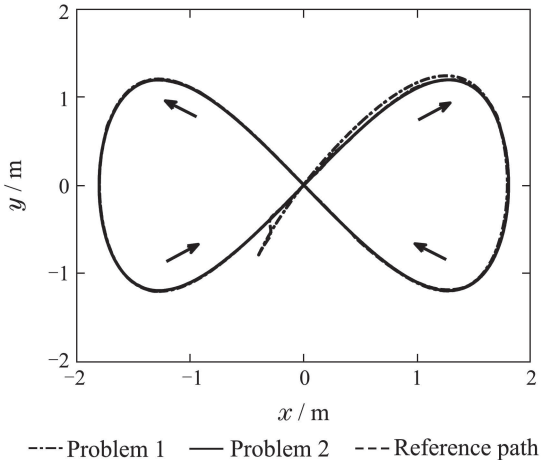

Fig. 2 The trajectories of problem 1, problem 2 and reference path

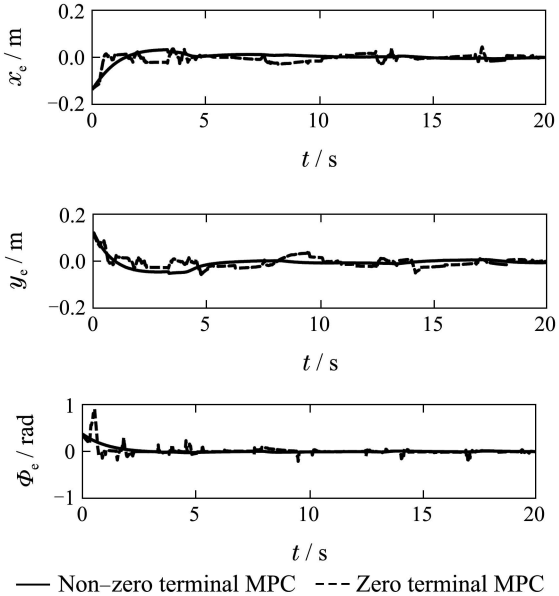

Fig. 3 Comparison of the error states

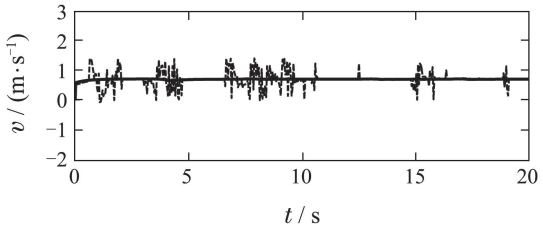

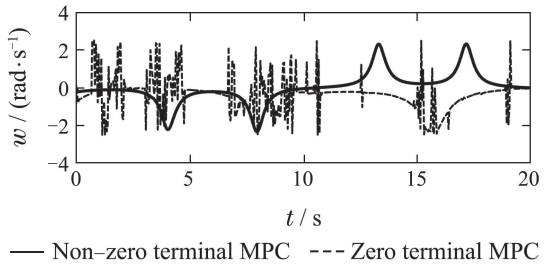

Fig. 4 Comparison of the control inputs

Table 3 Comparison of the computation burden

Computation time	Non-zero terminal	Zero terminal
In total/s	151.22	8845.86
Each step/s	0.1512	118.46

4.2 Nonsmooth path

The second path is a nonsmooth path

$$x_R = 1.8\sin\theta,$$
$$y_R = \begin{cases} 1.2\sin(2\theta), & 0 \leqslant \theta \leqslant \theta_k, \\ 1, & \theta > \theta_k, \end{cases} \tag{37}$$

where θ_k is a specific chosen path parameter.

Because Eq.(37) is a nonsmooth path, it is only applicable to test the performance of MPC scheme with zero terminal region. The simulation results are shown in Figs.5–7.

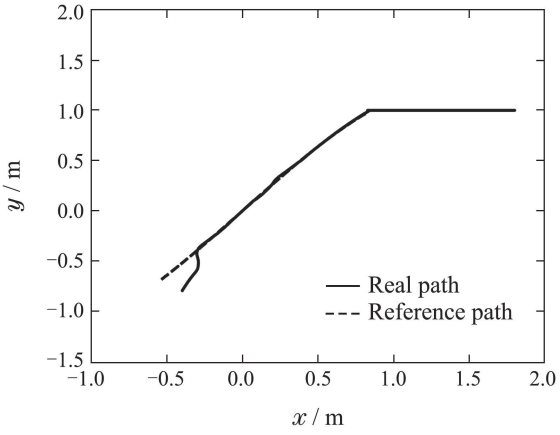

Fig. 5 The trajectories of real path and reference path

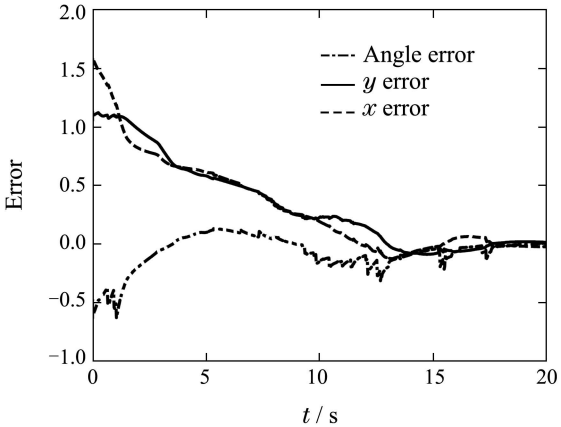

Fig. 6 The error states: angle error (rad), y error (m) and x error (m)

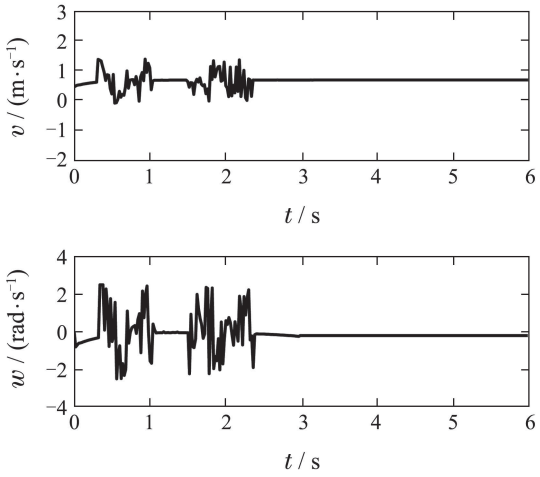

Fig. 7 The control inputs

From Figs.5–7, it can be seen that the MPC scheme with terminal equality constraints could also drive the robot to follow the reference path with admissible inputs. Note that the robot has already followed the given path before entering the second part of it.

4.3 Circle path

The third path is a circle, which is defined as

$$x_R = 1.2\cos\theta,\ y_R = 1.2\sin\theta. \tag{38}$$

The simulation results are shown in Figs.8–10. Compared with MPC with non-zero terminal region, MPC with zero terminal region can achieve similar control performance: the states of the robot have errors at the preliminary stage, the real path could converge finally to the reference circle path. The control inputs stay in the admissible range for the two controllers.

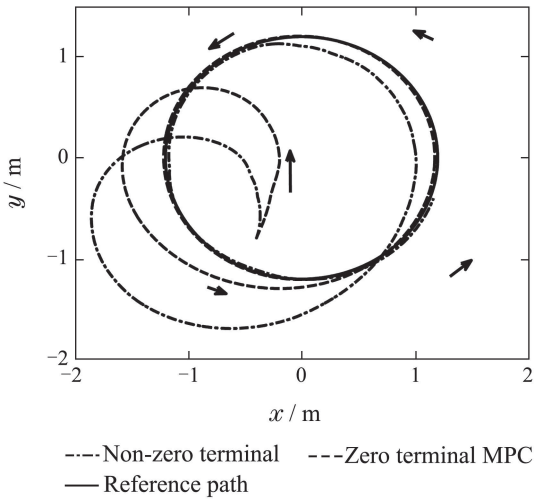

Fig. 8 The trajectories of non-zero terminal, zero terminal MPC and reference path

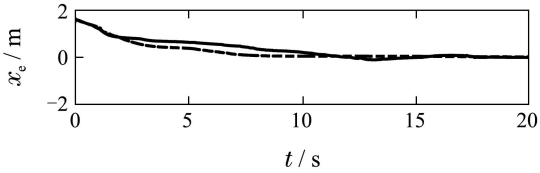

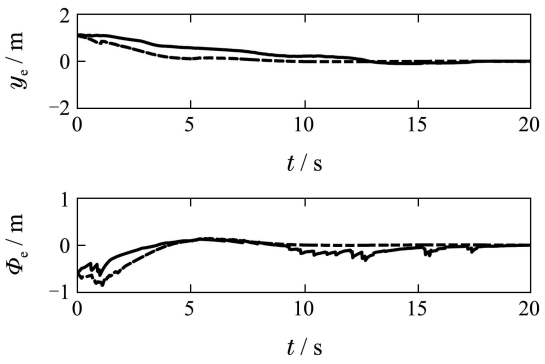

Fig. 9 Comparison of the error states: non-zero terminal MPC and zero terminal MPC

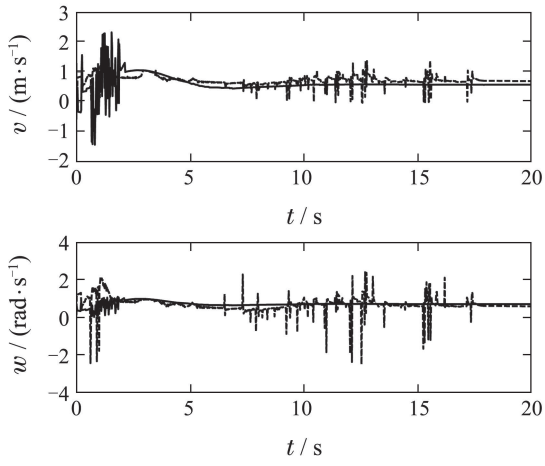

Fig. 10 Comparison of the control inputs: non-zero terminal MPC and zero terminal MPC

The real path based on zero terminal region converges to the reference circle faster, but the computational burden is much heavier as shown in Table 4.

Table 4 Comparison of the computation burden

Computation time	Non-zero terminal	Zero terminal
In total/s	393.75	4258.84
Each step/s	0.3937	92.75

The above simulations show that the robot has the ability to follow the reference path with high accuracy once it is on the reference. MPC with zero terminal region, by choosing the reference path as the terminal region, is an effective way for the path following problems of wheeled mobile robots. It can avoid complex calculation of the terminal ingredients and achieve similar performance compared with MPC with non-zero terminal region.

5 Conclusions

Model predictive control for path following problems of wheeled mobile robots was discussed in this paper, where the reference path was chosen as the terminal region. The optimization problem of MPC and sufficient conditions for convergence to the reference path were discussed. Simulation results were provided which show asymptotic convergence of the proposed scheme. Robots under model predictive control with zero terminal region can follow the given path under the admissible inputs. Although the computational burden is heavier than the conventional schemes, zero terminal region can achieve a smaller following error and is applicable to non-smooth paths.

References:

[1] CHEN H, ALLGÖWER F. A quasi-infinite horizon nonlinear model predictive control scheme with guaranteed stability [J]. *Automatica*, 1998, 34(10): 1205 – 1217.

[2] GUERREIRO B J, SILVESTRE C, CUNHA R, et al. Trajectory tracking nonlinear model predictive control for autonomous surface craft [J]. *IEEE Transactions on Control Systems Technology*, 2014, 22(6): 2160 – 2174.

[3] FAULWASSER T, KERN B, FINDEISEN R. Model predictive path-following for constrained nonlinear systems [C] //*Proceedings of the 48th IEEE Conference on Decision and Control Held Jointly with the 2009 28th Chinese Control Conference CDC/CCC 2009*. Shanghai, China: IEEE, 2009: 8642 – 8647.

[4] LIN X, JOUFFROY J. Modeling and nonlinear heading control of sailing yachts [J]. *IEEE Journal of Oceanic Engineering*, 2014, 39(2): 256 – 268.

[5] GU D, HU H. Receding horizon tracking control of wheeled mobile robots [J]. *IEEE Transactions on Control Systems Technology*, 2006, 14(4): 743 – 749.

[6] LI Z, LI J, KANG Y. Adaptive robust coordinated control of multiple mobile manipulators interacting with rigid environments [J]. *Automatica*, 2010, 46(12): 2028 – 2034.

[7] RACHAH A, NOLL D. Modeling and control of a semi-batch cooling seeded crystallizer [C] //*Proceedings of the 6th International Conference on Modeling, Simulation, and Applied Optimization (ICMSAO)*. Beijing, China: IEEE, 2015, 5: 1 – 6.

[8] HASSANZADEH M, LIDBERG M, KESHAVARZ M, et al. Path and speed control of a heavy vehicle for collision avoidance maneuvers [C] //*Intelligent Vehicles Symposium Alcalάde Henares*. Alcalάde Henares, Spain: IEEE, 2012: 129 – 134.

[9] LI X, SUN Z, ZHU Q, et al. A unified approach to local trajectory planning and control for autonomous driving along a reference path [C] //*Proceedings of IEEE International Conference on Mechatronics and Automation*. Tianjin, China: IEEE, 2014: 1716 – 1721.

[10] AKHTAR A, NIELSEN C, WASLANDER S. Path following using dynamic transverse feedback linearization for car-like robots [J]. *IEEE Transactions on Robotics*, 2015, 31(2): 269 – 279.

[11] SADOWSKA A, HUIJBERTS H. Formation control design for car-like nonholonomic robots using the backstepping approach [C] //*European Control Conference (ECC)*. Zürich, Switzerland: IEEE, 2013, 7: 1274 – 1279.

[12] XU D, LIAO Y, PANG Y, et al. Backstepping control method for the path following for the underactuated surface vehicles [C] //*Proceedings of 32nd Chinese Control Conference (CCC)*. Xi'an, China: IEEE, 2013, 7: 4188 – 4193.

[13] YANG Z, WANG Y, LIU F, et al. Path following of underactuated surface vessels based on neural sliding mode [C] //*Proceedings of the 33rd Chiese Control Conference (CCC)*. Beijing, China: IEEE, 2014, 8: 7858 – 7863.

[14] REZAPOUR E, PETTERSEN K Y, LILJEBÄCK P, et al. Differential geometric modeling and robust path following control of snake robots using sliding mode techniques [C] //*Proceedings of 2014 IEEE International Conference on Robotics and Automation (ICRA)*. Hong Kong, China: IEEE, 2014, 5: 4532 – 4539.

[15] LI Z, SU C, WANG L, et al. Nonlinear disturbance observer design for a robotic exoskeleton incorporating fuzzy approximation [J]. *IEEE Transactions on Industrial Electronics*, 2015, 62(9): 5763 – 5775.

[16] LI Z, YANG C, SU C, et al. Decentralized fuzzy control of multiple cooperating robotic manipulators with impedance interaction [J]. *IEEE Transactions on Fuzzy Systems*, 2015, 23(4): 1044 – 1056.

[17] HE W, DONG Y, SUN C. Adaptive neural impedance control of a robotic manipulator with input saturation [J]. *IEEE Transactions on Systems, Man, and Cybernetics: Systems*, 2016, 46(3): 334 – 344.

[18] HE W, DAVID A, YIN Z, et al. Neural network control of a robotic manipulator with input deadzone and output constraint [J]. *IEEE Transactions on Systems, Man, and Cybernetics: Systems*, 2016, 46(6): 759 – 770.

[19] RAWLINGS J B, MAYNE D Q. *Model Predictive Control: Theory and Design* [M]. Nob Hill Publishing: Madison, Wisconsin, 2009.

[20] MAYNE D Q, RAWLINGS J B, RAO C V, et al. Constrained model predictive control: stability and optimality [J]. *Automatica*, 2000, 36(6): 789 – 814.

[21] LIU X, CONSTANTINESCU D, SHI Y. Robust model predictive control of constrained non-linear systems: adopting the non-squared integrand objective function [J]. *IET Control Theory and Applications*, 2015, 9(5): 649 – 658.

[22] LIMON D, ALVARADO I, CAMACHO E F. MPC for tracking piecewise constant reference for constrained linear systems [J]. *Automatica*, 2008, 44(9): 2382 – 2387.

[23] JANG J T, MOON S T, HAN S, et al. Trajectory generation with piecewise constant acceleration and tracking control of a quadcopter [C] //*Proceedings of IEEE International Conference on Industrial Technology*. Seville, Spain: IEEE, 2015, 5: 530 – 535.

[24] FAULWASSER T, FINDEISEN R. Constrained output path-following for nonlinear systems using predictive control [C] //*Proceedings of the 8th IFAC Symposium on Nonlinear Control Systems*. Bologna, Italy: [s.n.], 2010, 9: 753 – 758.

[25] HLADIO A, NIELSON C, WANG D. Path following controller design for a class of mechanical systems [J]. *IEEE Transactions on Control Systems Technology*, 2013, 21(6): 2380 – 2390.

[26] MARAFIOTI G, LILJEBÄCK P, TRANSETH A A. A study of nonlinear model predictive control (NMPC) for snake robot path following [C] //*Proceedings of the 2014 IEEE International Conference on Robotics and Biomimetics*. Bali, Indonesia: [s.n.], 2014, 12: 568 – 573.

[27] YU S, CHEN H, ZHANG P, et al. An LMI optimization approach for the terminal region of MPC for nonlinear systems [J]. *Acta Automatica Sinica*, 2008, 34(7): 798 – 804.

[28] RAWLINGS J B, MUSKE K R. Stability of constrained receding horizon control [J]. *IEEE Transactions on Automatic Control*, 1993, 38(10): 1512 – 1516.

[29] CHENG Y. *Trajectory planning of wheeled mobile robot based on differential flatness* [D]. Changchun: Jinlin University, 2008.

[30] YU S, LI X, CHEN H, et al. Nonlinear model predictive control for path following problem [J]. *International Journal of Robust and Nonlinear Control*, 2014, 25(8): 1168 – 1182.

[31] YU S, HOU C, QU T, et al. A revisit to MPC of discrete-time nonlinear systems [C] //*Proceedings of the 5th Annual IEEE International Conference on Cyber Technology in Automation, Control and Intelligent Systems*. Shenyang, China: IEEE, 2015: 7 – 12.

作者简介:

刘　洋　(1991–), 女, 硕士, 智能安全专业工程师, 目前研究方向为智能汽车轨迹规划和轨迹跟踪技术, E-mail: liuyang9407@126.com;

于树友　(1974–), 男, 副教授, 硕士生导师, 目前研究方向为模型预测控制的鲁棒性分析与综合、随机系统的模型预测控制算法, E-mail: shuyou@jlu.edu.cn;

郭　洋　(1989–), 女, 硕士研究生, 目前研究方向为轮式移动机器人的路径跟踪与干扰观测器的设计, E-mail: 861460929@qq.com;

高炳钊　(1977–), 男, 教授, 博士生导师, 目前研究方向为汽车动力传动系统控制与车辆稳定性控制, E-mail: gaobz@jlu.edu.cn;

陈　虹　(1963–), 女, 教授, 博士生导师, 目前研究方向为先进控制理论与技术、工业过程、机械车辆等系统的动力学仿真、性能评价及优化控制, E-mail: chenh@jlu.edu.cn.